

On the nature of amorphous polymorphism of water

M.M. Koza¹, B. Geil², K. Winkel², C. Köhler²,
F. Czeschka^{1,3}, M. Scheuermann² H. Schober¹, T. Hansen¹.

¹*Institut Laue-Langevin, F-38042 Grenoble Cedex, France.*

²*Institut für Festkörperphysik, TU-Darmstadt, Germany.*

³*Institut für Festkörperphysik, TU-München, Germany.*

(Dated: July 6, 2021)

Abstract

We report elastic and inelastic neutron scattering experiments on different amorphous ice modifications. It is shown that an amorphous structure (HDA') indiscernible from the high-density phase (HDA), obtained by compression of crystalline ice, can be formed from the very high-density phase (vHDA) as an intermediate stage of the transition of vHDA into its low-density modification (LDA'). Both, HDA and HDA' exhibit comparable small angle scattering signals characterizing them as structures heterogeneous on a length scale of a few nano-meters. The homogeneous structures are the initial and final transition stages vHDA and LDA', respectively. Despite, their apparent structural identity on a local scale HDA and HDA' differ in their transition kinetics explored by *in situ* experiments. The activation energy of the vHDA-to-LDA' transition is at least 20 kJ/mol higher than the activation energy of the HDA-to-LDA transition.

PACS numbers: 61.12.-q,61.43.Fs,64.60.My,64.70.Kb

Amorphous polymorphism is strongly linked to water, where for the first time two distinct amorphous modifications, namely a high-density amorphous (HDA, $\rho \approx 39$ mol./nm³) and a low-density amorphous (LDA, $\rho \approx 31$ mol./nm³) ice state could be prepared [1]. The existence of HDA and LDA and the characteristics of the transition between these two modifications, often referred to as first-order like, have triggered major experimental and theoretical efforts that all aim for a conclusive explanation of amorphous polymorphism [2]. It has, in particular, been conjectured from Molecular Dynamics (MD) simulations, that water in the super-cooled region exhibits a second critical point and a first-order transition line separating two liquid phases towards lower temperatures [3]. In this picture HDA and LDA are supposed to be glassy representatives of these two liquids.

The scenario of two super-cooled liquid phases has been recently questioned by the discovery of a third disordered modification apparently distinct from HDA and LDA and called, due to its higher density ($\rho \approx 41$ mol./nm³), very high-density amorphous (vHDA) ice [4]. Moreover, latest computer simulations are in apparent agreement with this finding suggesting the presence of "multiple liquid-liquid transitions in super-cooled water" [5].

Amorphous systems like liquids are isotropic and thus possess by definition no particular global symmetry. In the glassy state they are in addition non-ergodic, i.e. they are prone to relax their structures following distinct energetic pathways that may or may not be accessible during the experiment. Thus, unless there are clear indications for thermodynamic transitions, it is not possible to assign distinct phases to an amorphous system. The evolution of an amorphous system as a function of temperature, pressure and time may, however, be characterized via the changes encountered in local structural units. These can e.g. be studied with wide-angle diffraction. If the structural changes are significant this approach allows for a characterisation of the amorphous states. We would like to recall that due to the non-ergodic nature of the sample what we call a state is not necessarily completely characterized by thermodynamic variables but may well depend on the sample history. In the case of water the nearest-neighbor coordination number has been proposed as a criterium to distinguish LDA, HDA and vHDA (coordination number of four, five and six, respectively) [6, 7]. Another approach recently used in MD simulations bases the analysis not on the coordination number but on the ring structures encountered in the system [8]. The important question remains whether the local characterization is sufficient and whether the thus classified states actually correspond to distinct phases.

In this communication we present diffraction and inelastic neutron scattering experiments on both HDA and vHDA samples. HDA (D_2O) has been formed by slow compression of crystalline ice I_h to 18 kbar at 77 K [9]. vHDA samples have been obtained by heating HDA (D_2O) samples at high pressure [4]. Here, we present data collected with three vHDA samples formed at $p = 10.5$ kbar $T = 145$ K # 1, $p = 10.5$ kbar $T = 155$ K # 2 and $p = 16$ kbar $T = 155$ K # 3. After the vHDA structure is formed all samples are cooled at the indicated p to $T = 77$ K and retrieved from the pressure cells, crushed into mm-sized chunks and placed into proper sample containers. Please note, that throughout this paper we will refer to the amorphous ice modifications obtained from vHDA by heating as HDA' and LDA'. We will show that HDA and HDA', a modification of amorphous ice obtained by heating of vHDA at ambient p , are indistinguishable in terms of local structure and dynamics as probed in reciprocal space by neutron scattering. The amount of small angle scattering gives evidence that HDA and HDA' are both heterogeneous structures.

Diffraction experiments have been carried out at the high-flux instrument D20 ($\lambda = 2.4$ Å and 1.3 Å) and inelastic data have been collected at the time-of-flight spectrometer IN6 ($\lambda = 4.1$ Å), Institut Laue-Langevin, Grenoble, France. Standard data corrections for empty container scattering (IN6) and detector calibration of both instruments, has been applied. Elastic data are normalized to the coherent part of the IN6 response allowing a comparison of all data sets with each other [10]. The *in situ* transformations of vHDA into LDA' have been followed in an Helium atmosphere of 200 mbars, and the corresponding data evaluation have been carried out according to reference [11]. 1–2 mbars of Helium pressure have been applied during the inelastic experiments.

The static structure factor $S(Q)$ of sample # 2 is reported in Fig. 1. $S(Q)$ of HDA and vHDA is measured at 75 K, that of HDA' is obtained during *in situ* annealing at 113 K. $S(Q)$ of LDA' is determined after annealing at 135 K. Fig. 1 demonstrates that it is possible to select an intermediate ice modification HDA' such that the $S(Q)$ of HDA' and HDA coincide. It furthermore can be shown that to any modification encountered along the transition from HDA to LDA [11] we find a matching partner along the transition from vHDA to LDA'. In terms of $S(Q)$ the transition states of HDA to LDA appear as a subset of the transition states of vHDA to LDA'. Characteristic features of both transitions are the continuous down-shift of the maximum in $S(Q)$ and the transient broadening of the intermediate maximum, which shows the largest width in the middle of the transition [11, 12]. This is demonstrated in

the insert of Fig. 1 by the $S(Q)$ of vHDA, HDA' and an intermediate state identified as the state of strongest heterogeneity (SSH), as it is discussed below.

The initial transition stage is a matter of the thermodynamic conditions, i.e. p and T , during sample preparation. This point is substantiated equally in the insert of Fig. 1 where the main peak of $S(Q)$ is plotted for samples # 1, # 2 and # 3. vHDA of sample # 1 appears as an apparent intermediate state between vHDA and HDA' measured with sample # 2. It can be matched by an intermediate $S(Q)$ of sample # 2 transforming into LDA'. The sample preparation concerning p and T is fully reproducible, however we cannot exclude that the final state obtained is conditioned by the history, i.e. by the state of relaxation of the sample at the time when p and T were applied.

Another basic characteristic of the transitions is a transient enhancement of $S(Q)$ at $Q \leq 0.6 \text{ \AA}^{-1}$. Figs. 2 a and 2 b report on the $S(Q)$ determined with sample # 1 in the states vHDA, HDA' and LDA' and a HDA sample at IN6 and with sample # 2 in the states vHDA, HDA', LDA' and the state of strongest heterogeneity (SSH) at D20, respectively. The striking feature is that HDA, as an initial state, and HDA', as an intermediate state, show a clear enhancement at $Q \leq 0.6 \text{ \AA}^{-1}$. This enhancement is absent in vHDA and LDA' and as reported by us in references [13, 14] it is equally missing in LDA. The low- Q signal gives evidence for the heterogeneous nature of the states that in terms of the wide-angle $S(Q)$ are intermediate to vHDA and LDA'. This holds no matter how the intermediate modifications were obtained in our experiments.

The enhanced signal in the low- Q range coincides well with the behaviour of the wide-angle $S(Q)$. This is directly demonstrated by the broadening of the structure factor maximum in the raw data (Fig. 1). It can also be visualized by computing the Fourier transform $D(r)$ of $S(Q)$ shown in Fig. 2 c [15]. Obviously, in contrast to the properties of vHDA and LDA' oscillations in $D(r)$ of SSH are strongly suppressed beyond $r > 10 \text{ \AA}$, indicating an apparent reduction of spatial correlations in the intermediate states. Please note, that variation of the signal at $Q < 0.65 \text{ \AA}^{-1}$ have been suppressed for the computation of the data shown in Fig. 2 c, thus, leaving $D(r)$ unperturbed by the low- Q regime.

The one-to-one correspondance of vHDA-to-LDA' and HDA-to-LDA states does not only hold for the elastic signal but is equally observed for molecular vibrations. In Fig. 3 a we report the direct time-of-flight signal $I(2\Theta, \text{tof})$ measured at 75 K with sample # 1 at IN6 and averaged over the 2Θ range sampled by the spectrometer. Fig. 3 b shows the

corresponding generalized density of states $G(\omega)$. It is obvious that no significant difference can be detected in the spectra of HDA and HDA'. The characteristic maximum in $G(\omega)$ which is due to low-energy optic modes in the crystalline counterparts shifts towards lower energies when vHDA transforms into LDA' and the sample density decreases, a feature as well observed for the diversity of crystalline phases [16, 17]. Within the accuracy of the experiments the $G(\omega)$ of vHDA does not show any fingerprints of H-bond penetration, whose effect on the inelastic response should result in a pronounced splitting of the strong maximum.

The fact that HDA and HDA' are identical in terms of $S(Q)$ and $G(\omega)$ poses the question of their likeness in the framework of thermodynamics. To explore this point *in situ* experiments of the transition vHDA to LDA' have been performed on sample #2 (5 portions of ~ 0.5 ml each) at temperatures 109 K, 113 K, 114 K, 115.5 K and 117 K. Fig. 4 shows the evolution of $S(Q)$ in the wide angle $I_w(t, T)$ (top figure) and small angle $I_s(t, T)$ (bottom figure) regime [18]. By definition, $I_w(t, T)$ equals 1 for vHDA and zero for LDA'. Indicated as the grey shaded area is the stage of the transition at which HDA' is identified. It becomes immediately clear that at a given temperature vHDA transforms into LDA' on a longer time scale than HDA converts into LDA. The characteristic time constants $\tau(T)$ of the transition follow an Arrhenius line with an activation energy $\Delta E \approx 65$ kJ/mol, i.e., a ΔE of at least 20 kJ/mol higher than for the HDA to LDA transition [11]. In other words, HDA' is structurally stable in the temperature range in which HDA transforms rapidly to LDA.

By combining a logarithmic term, which takes care of aging [19], with an Avrami-Kolmogorov expression, which describes a first-order transition, it is possible to reproduce $I(T, t)$ analytically for the HDA to LDA transition [11]. This is not the case when starting the annealing process from vHDA. As can be seen from fig.4 the transition from HDA' to LDA' becomes nearly uncontrollable at any temperature once it has set in. Such a rapid transition kinetics is *a priori* incompatible with the higher activation energy found for $\tau(T)$ when the system is in equilibrium. Therefore, an additional energy scale must be at work. Given the speed of the transition the evacuation of latent heat from the sample and thus the temperature control becomes a real experimental challenge.

Indeed, following the vHDA to LDA' transition in high-vacuum the vHDA samples re-crystallize directly. In contrast, LDA can be at any pressure obtained from HDA. This be-

haviour can be easily understood by comparing the activation energies of the vHDA to LDA' transition with the activation energy ≈ 66 kJ/mol of recrystallisation of hyper-quenched glassy water [20]. This shows that the vHDA to LDA' transition energy is very close to the recrystallisation limit of low-density amorphous ice modifications.

In summary, we have shown that HDA, produced by compression of hexagonal ice I_h , and HDA', obtained as an intermediate phase in the course of the transition vHDA to LDA', give indiscernible responses in elastic and inelastic neutron scattering experiments. A pronounced and transient low- Q signal gives evidence for heterogeneity in both HDA and HDA'. They thus are similar beyond the local structural level. Despite the fact that HDA and HDA' are indiscernible in terms of their $S(Q)$ and $G(\omega)$ they are energetically not identical as shown by the differences in transition kinetics. It is not possible to tell from our experiments what properties are responsible for this energetic difference. However, it is reasonable to conjecture that the inequality holds as well for the final transition states LDA and LDA' [21, 22].

The resemblance of the HDA and HDA' response functions shows unequivocally that static experiments probing local properties in reciprocal space, here in particular wide angle diffraction, are insufficient to fully characterize the non-ergodic system. The existence of a transient low- Q diffraction signal demonstrates the importance of collecting information in a region of reciprocal space as large as possible to decide upon the spatial homogeneity of the samples. This does not hold only for experiments applying temperature as a control parameter, but includes any study using some external force, e.g. pressure [19], to which the non-ergodic sample is forced to respond. Resemblance in terms of homogeneity still does not mean that we deal physically with the same system. Only time depending experiments give us information on the energy states explored by the system [19, 23, 24]. In fact, HDA and HDA' are unequivocally different in this respect.

The present findings do in no way question the two-liquid scenario. The seemingly homogeneous structures vHDA and LDA' are good candidates for the glassy counterparts of the thermodynamic liquid states [3]. Concerning local structure both HDA' and HDA belong to the vHDA basin of states. The transition from vHDA to LDA' involves heterogeneous intermediate stages among which we find HDA'. It bears all signs of a phase transition including the abrupt nearly singular change of local structural order between HDA' and LDA'. No other transitions or transition stages justifying the presence of more than the

two homogeneous structures could have been identified [5]. As far as the properties of the wide-angle $S(Q)$ reported here and in reference [11] are concerned they are in agreement with recently published results from molecular dynamics simulations [8, 22]. A computation of the properties observed in $S(Q)$ in the low- Q range, however require a larger simulation box size than the one used.

-
- [1] O. Mishima, L. D. Calvert, and E. Whalley, *Nature* **310**, 393 (1984).
- [2] O. Mishima and H. E. Stanley, *Nature* **396**, 329 (1998).
- [3] P. H. Poole, F. Sciortino, T. Grande, H. E. Stanley, and C. A. Angell, *Phys. Rev. Lett.* **73**, 1632 (1994).
- [4] T. Loerting, C. Salzmann, I. Kohl, E. Mayer, and A. Hallbrucker, *Phys. Chem. Chem. Phys.* **3**, 5355 (2001).
- [5] I. Brovchenko, A. Geiger, and A. Oleinikova, *J. Chem. Phys.* **118**, 9473 (2003).
- [6] J. L. Finney, A. Hallbrucker, I. Kohl, A. Soper, and D. Bowron, *Phys. Rev. Lett.* **88**, 225503 (2002).
- [7] J. L. Finney, D. T. Bowron, A. K. Soper, A. Hallbrucker, T. Loerting, E. Mayer, and A. Hallbrucker, *Phys. Rev. Lett.* **89**, 205503 (2002).
- [8] R. Martonak, D. Donadio, and M. Parrinello, *Phys. Rev. Lett.* **92**, 225702 (2004).
- [9] M. M. Koza, H. Schober, T. Hansen, A. Toelle, and F. Fujara, *Phys. Rev. Lett.* **84**, 4112 (2000).
- [10] $S(Q)$ from IN6 data is obtained as:
- $$S(Q) = \int_{-\infty}^{+\infty} S(Q, \omega) d\omega.$$
- [11] M. M. Koza, H. Schober, H. E. Fischer, T. Hansen, and F. Fujara, *J. Phys.: Condens. Matter* **15**, 321 (2003).
- [12] M. Guthrie, J. Urquidi, C. A. Tulk, C. J. Benmore, D. D. Klug, and J. Neuefeind, *Phys. Rev. B* **68**, 184110 (2003).
- [13] H. Schober, M. M. Koza, A. Toelle, F. Fujara, C. A. Angell, and R. Boehmer, *Physica B* **241–243**, 897 (1998).
- [14] H. Schober, M. M. Koza, A. Toelle, C. Masciovecchio, F. Sette, and F. Fujara, *Phys. Rev. Lett.* **85**, 4100 (2000).

- [15] $D(r) \equiv \int_0^\infty (S(Q) - S(Q_{\max}))Q \sin(Q \cdot r)dQ$, with Q_{\max} the maximum accessed Q number. Spurious Bragg-peaks and arteficial detector spikes have been suppressed in $S(Q)$ data.
- [16] J. Li, J. Chem. Phys. **105**, 6733 (1996).
- [17] M. M. Koza, H. Schober, B. Geil, M. Lorenzen, and H. Requardt, Phys. Rev. B **69**, 024204 (2004).
- [18]
$$I_w(t, T) = \frac{\int_{0.6}^{2.75} |S(Q;LDA') - S(Q;t,T)|dQ}{\int_{0.6}^{2.75} |S(Q;LDA') - S(Q;vHDA)|dQ}.$$

$$I_s(t, T) = \frac{\int_{0.35}^{0.55} S(Q;t,T)dQ - \int_{0.35}^{0.55} S(Q;vHDA)dQ}{I_{\max}(t,T)},$$
with $I_{\max}(t, T)$ the maximum $\int_{0.35}^{0.55} S(Q; t, T)dQ$ observed during the respective *in situ* measurement.
- [19] V. Karpov and M. Grimsditch, Phys. Rev. B **48**, 6941 (1993).
- [20] W. Hage, A. Hallbrucker, E. Mayer, and G. Johari, J. Chem. Phys. **103**, 545 (1995).
- [21] N. Giovambattista, H. Stanley, and F. Sciortino, Phys. Rev. Lett. **91**, 115504 (2003).
- [22] B. Guillot and Y. Guissani, J. Chem. Phys. **119**, 11740 (2003).
- [23] F. Sciortino and P. Tartaglia, J. Phys.: Condens. Matter **13**, 9127 (2001).
- [24] N. Giovambattista, H. Stanley, and F. Sciortino, Phys. Rev. E **69**, 2004 (2004).

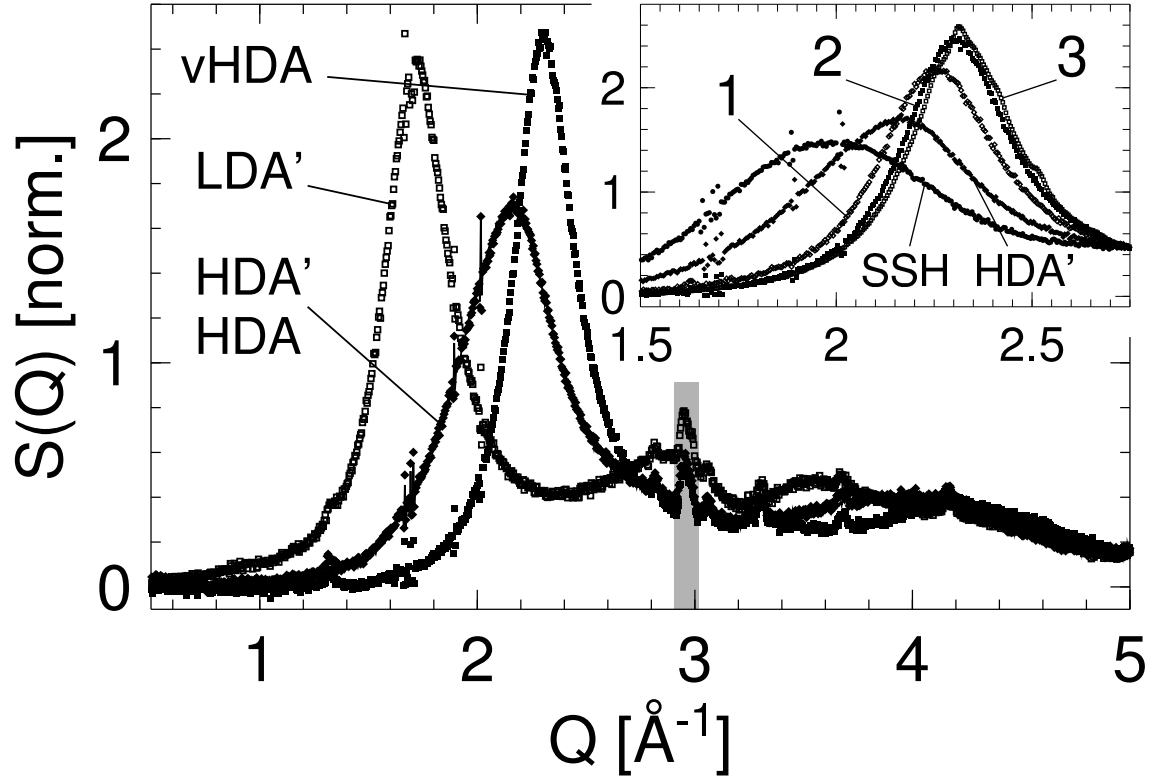


FIG. 1: Static structure factor $S(Q)$ of vHDA #2 (■), HDA' (◆) and LDA' (□), as obtained from vHDA #2, and of HDA (–), as produced by compressing ice I_h . Please note that HDA' and HDA are hardly distinguishable. The grey shaded area indicates a Bragg-peak from the sample container. The insert reports the maximum of $S(Q)$ for vHDA samples #1, #2 and #3. Equally shown are HDA' and SSH #2.

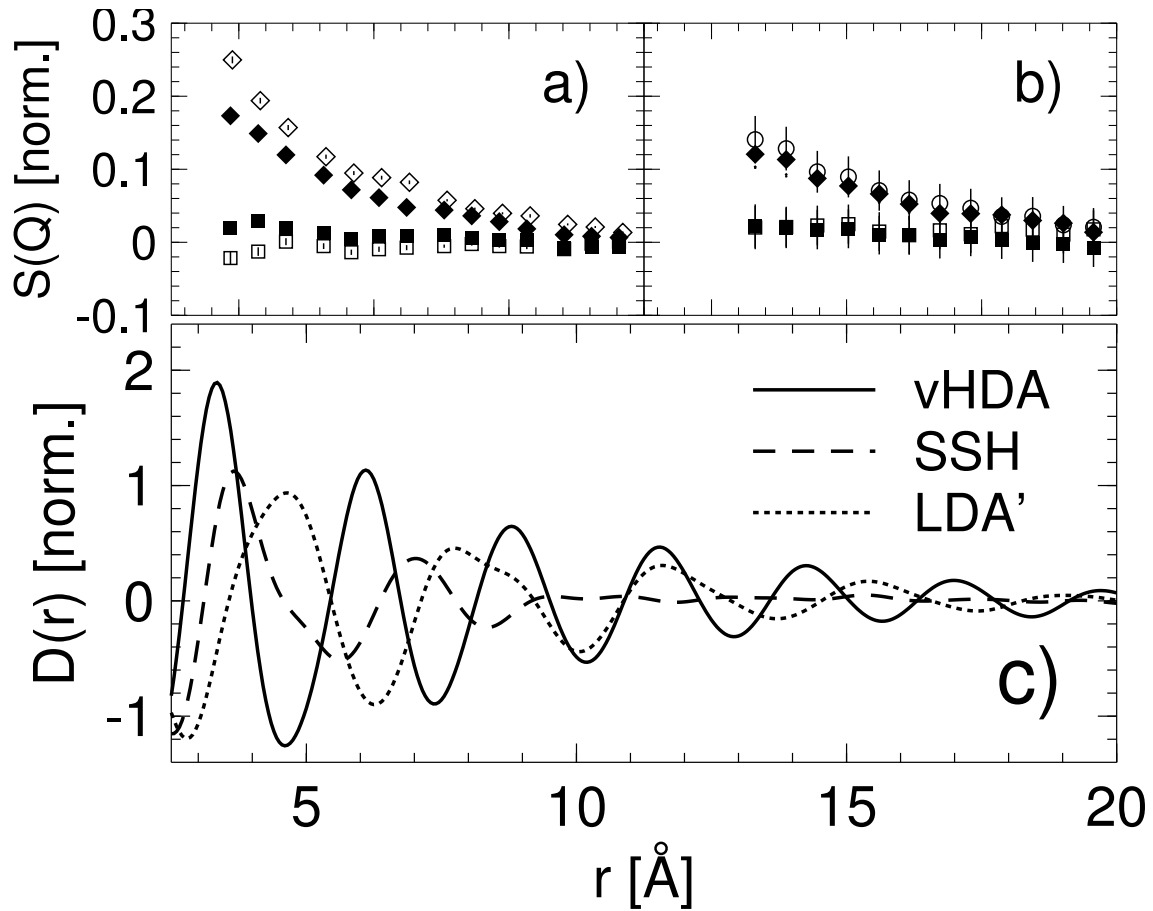


FIG. 2: (a) $S(Q)$ small angle signal of vHDA (■), LDA' (□), HDA' (◆) and HDA (◇) measured at IN6 and (b) of vHDA (■), LDA' (□), HDA' (◆) and SSH (○) measured at D20 (# 2 in Fig. 1). (c) $D(r)$ calculated for vHDA, LDA' and SSH from Fig. 1.

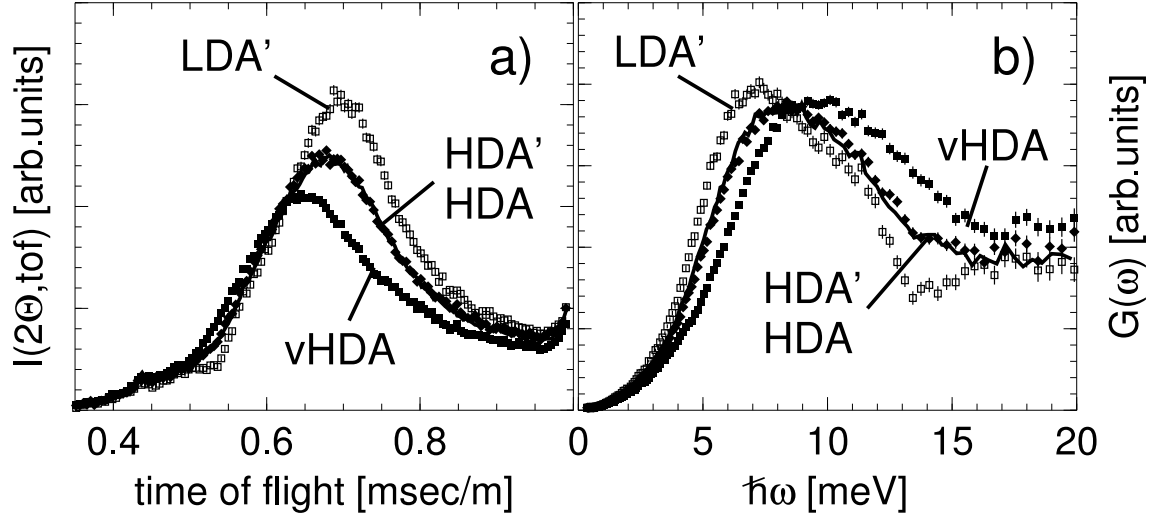


FIG. 3: (a) Inelastic intensity and (b) calculated generalized density of states $G(\omega)$ measured at $T = 75$ K at the spectrometer IN6.

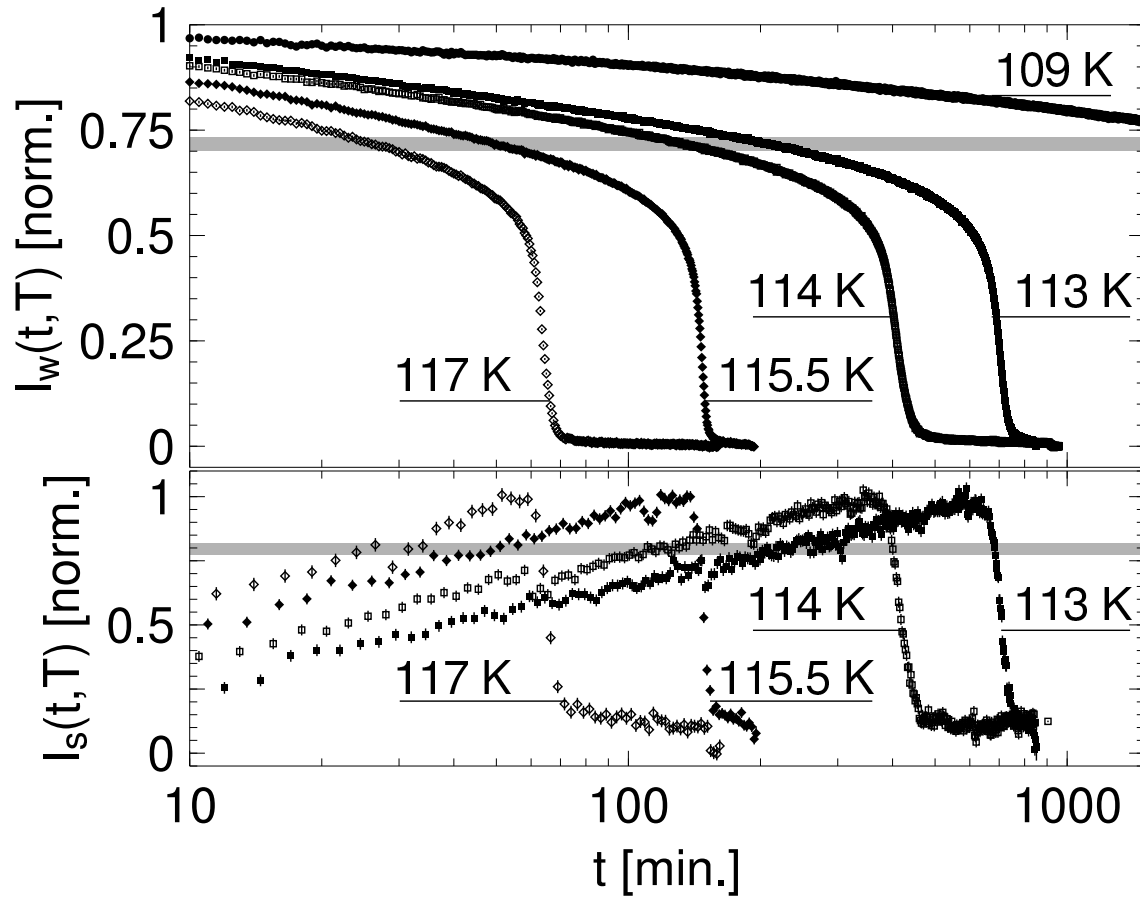


FIG. 4: On top, kinetics of the vHDA into LDA' transition determined with sample #2 shown in Fig. 1. The nominal temperatures are given in the figure. The grey shaded area indicates the position of HDA' and respectively HDA in the plot. At bottom, kinetics of the transient intensity at low- Q shown in Fig. 2 b.